Date: November 11, 1988

TITLE: COMPUTER-AIDED MOLECULAR DESIGN OF METHANE-ACTIVATION CATALYSTS

PI: J. A. Shelnutt

INSTITUTION/ORGANIZATION: Fuel Science Division 6211
Sandia National Laboratories
Albuquerque, NM 87185
Phone: 505-844-8856

PERIOD OF PERFORMANCE: FY86-FY89

OBJECTIVE: To develop a methodology for computer-aided molecular design of catalysts. Emphasis is on the design of biomimetic catalysts for alkane activation, with specific emphasis on methane-to-methanol conversion.

TECHNICAL APPROACH: A methodology for developing new catalysts using computer-aided molecular design (CAMD) techniques is being developed and applied to selective alkane hydroxylation. An iterative procedure for designing catalysts includes several tasks: (1) investigation of enzymes to learn what structural features to build into the synthetic catalyst; (2) use of CAMD methods to find synthesizable catalysts with the required molecular features; (3) synthesis of potential catalysts identified in the CAMD studies; (4) structural and chemical characterization of the synthetic catalysts to verify that the molecular structures are those desired; and (5) measurements of catalytic activity and stability of the designed catalysts. The structural characterization and catalytic activity determinations provide information from which the CAMD predictions can be evaluated. More importantly, the resulting structure-activity relationships give a basis for further improvements in catalyst design.

Biomimetic Alkane Oxidation. Our design activities are guided by structural and chemical information about naturally occurring biological catalysts such as cytochrome P_{450}, methyl reductase, methyl transferase, and methane monooxygenase. Specifically, cytochrome P_{450} carries out the hydroxylation of many hydrocarbons. The active site of P_{450} contains an iron porphyrin. The P_{450} reaction cycle is illustrated in Figure 1. Since the reaction occurs at ambient temperature and pressure, two one-electron reductions are required to activate O_2 resulting in the reactive intermediate, an oxo-iron(IV) porphyrin radical cation. (In high-temperature direct conversion, a reductant is not required to activate O_2.) This intermediate then reacts with the bound alkane inserting the Fe bound oxygen atom in the alkane C-H bond, and regenerating the starting Fe(III)-porphyrin catalyst. (In some biomimetic reactions, we use single oxygen atom donors, such as iodosylbenzene, NaOCl, and others, to generate the reactive Fe=O intermediate without having to provide a reductant or O_2.)

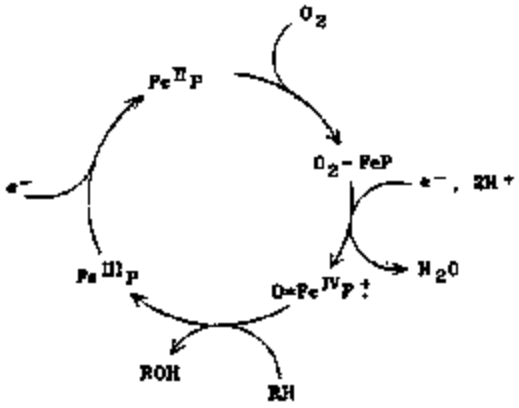

CYTOCHROME P_{450} HYDROCARBON-OXIDATION CYCLE

Figure 1.

The catalytic site in cytochrome P_{450} illustrates some of the structural features that are important in biological alkane oxidation and which may be useful in designing our synthetic catalysts. As can be seen from the crystal structure[1] of P_{450} shown in Figure 2, the active Fe center is embedded deep within the protein matrix. The active site also has, adjacent to the Fe porphyrin, a pocket of a size and shape suited for binding the substrate molecule (camphor in this case). Having the active site buried deep in the protein provides selective access of the substrate molecule to the catalytic center, thereby preventing oxidation of other system components, including P_{450} itself. This insures the stability of the catalytic system as a whole.

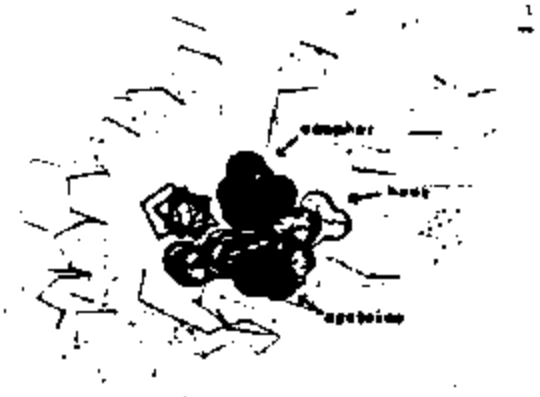

Figure 2

Figure 2 also shows that the Fe porphyrin is bound at the active site by a thiolate sulfur coordinated to the Fe at an axial ligation position. The sulfur ligand is thought to promote the formation of the reactive Fe=O species by making lysis of the O-O bond easier. Therefore, providing a

suitable axial ligand is a desired structural feature for our synthetic catalyst.

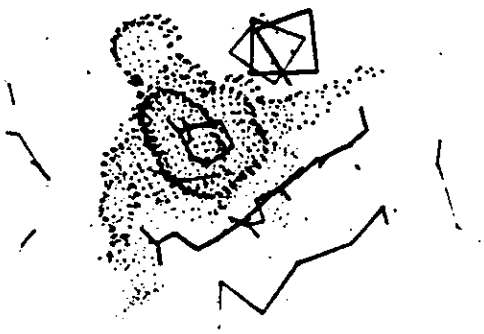

Figure 3.

Closer examination of the catalytic site as shown in Figure 3 points out the necessity of a good lock-and-key fit between the substrate and the binding cavity. This is especially true if a specific carbon atom of the substrate is to be selectively hydroxylated. In addition, the pocket gives the enzyme high affinity for its substrate. The driving forces for substrate binding are the hydrophobic and van-der-Waals interactions. Thus, in a polar solvent an aliphatic pocket of the size and shape of the substrate is a desirable structural feature.

The crystal structure of cytochrome P_{450} in the absence of the camphor molecule shows that the pocket is rigid. That is, instead of collapsing the cavit fills with water molecules. The rigidity of the pocket serves two purposes. First, it increases the affinity for the substrate. And, second, it provides catalyst stability by preventing internal oxidation of the protein immediately surrounding the active site.

It is desirable to design all of these features into a synthetic catalyst which mimics the P_{450} reaction, but which is designed for a chosen substrate molecule. Metalloporphyrins provide a unique molecular structure for construction of tailored catalysts. Also, over 70 metals have been inserted into porphyrins and Fe, Mn, Ru, and Rh have been shown to catalyze alkane oxidation reactions. Besides providing the catalytic metal center, the porphyrin macrocycle serves as a platform upon which additional molecular architecture is erected to provide the structural features required to mimic the size and shape selectivity of the enzyme. A variety of peripheral substituents are possible for construction of the binding cavity. Peripheral substituents can be used to modify the properties of the metal incorporated into the porphyrin ring. Substituents can also be used to control solubility or to attach the metalloporphyrin catalyst to a support.

Computer-Aided Molecular Design. We are using molecular mechanics calculations to evaluate new molecular designs based on metalloporphyrins. Our efforts to design and synthesize biomimetic catalysts for methane oxidation are based on tetraphenyl porphyrin, shown in Figure 4.

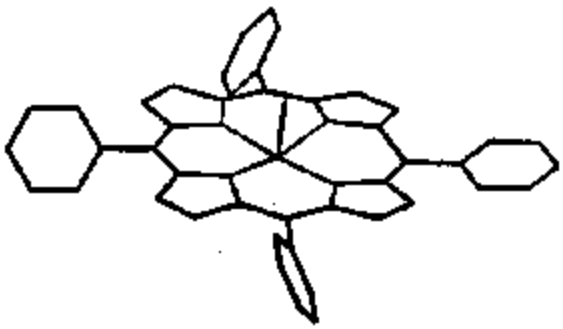

Figure 4.

Using this basic structure as a starting point substituents are added to the phenyl rings to generate a binding cavity at the metal center. An example is the carboranyl derivative shown in Figure 5.

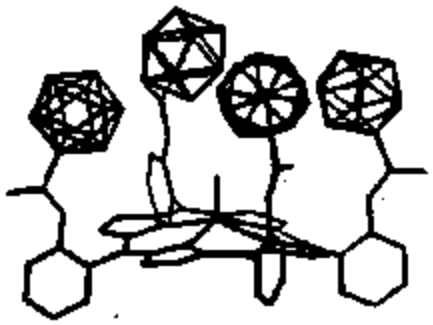

Figure 5.

The deep-pocket porphyrin shown has a cavity not much larger than the bound oxygen atom. The cavity is formed by the carborane cages, the amide linkages to the ortho-positions of the phenyl rings, and the porphyrin macrocycle itself. The size of the cavity formed is best perceived when the van-der-Waals surface of the atoms is displayed as in the dot surface of Figure 6.

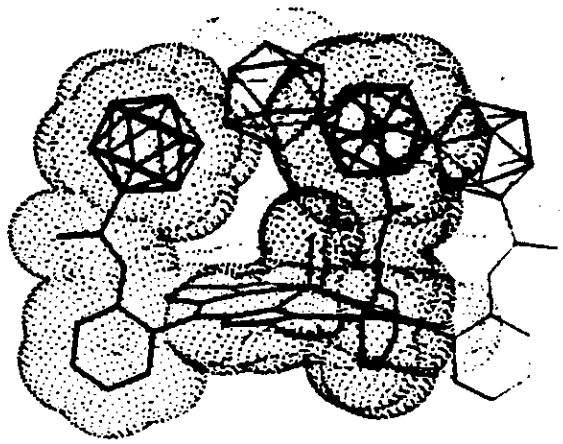

Figure 6.

As can be seen from Figure 6 it will be difficult to get both oxygen and methane into the pocket of this carboranyl porphyrin. An improved catalyst structure might include an extra atom in the amide link, thus providing a slightly larger cavity as shown in Figure 7.

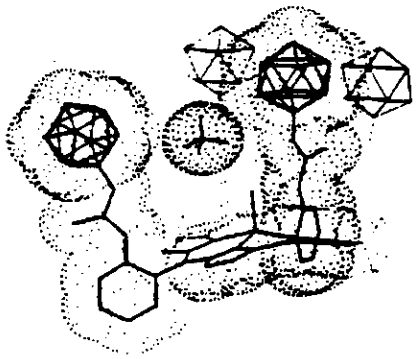

Figure 7.

This illustrates the usefulness of simple molecular graphics techniques in designing catalysts. However, more sophistocated molecular mechanics methods can help to further evaluate such hypothetical structures. For example, energy minimization of the structure shown in Figure 7 with a methane molecule positioned in the pocket demonstrates that binding of methane in the cavity is not unfavorable energetically. Such energy minimization calculations include the complete set of force constants (bonds, angles, torsions, etc.) of the molecules and the van-der-Waals, electrostatic, and hydrogen-bonding interactions between all atoms. A solvent cage can be generated around the molecule, and the molecular mechanics calculation made to include the interactions with the solvent, as

illustrated in Figure 8. The structures shown in Figures 7 and 8 are the result of such an energy-minimization calculation, but for simplicity Figure 7 does not show the solvent.

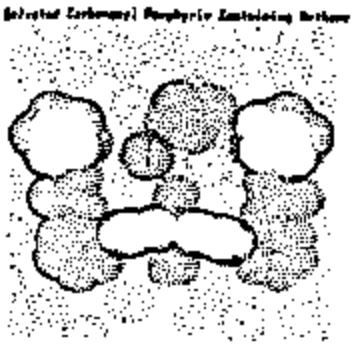

Figure 8.

An even more realistic picture of the interaction of the methane molecule with the cavity-containing, long-chain carboranyl porphyrin is obtained by carrying out a molecular dynamics calculation at 300° K. This allows the effect of the catalyst's motion on substrate binding to be evaluated at the specified temperature.

Figure 9.

Figure 9 shows the carboranyl porphyrin after 6 ps has elapsed at 300° K starting from the structure shown in Figures 7 and 8. By this time the methane molecule has moved out of the pocket. However, as shown in Figure 10, methane has moved back into the pocket by 7 ps. The molecular dynamics calculations suggest in a more meaningful way that the binding of methane is not unfavored energetically for the long-chain carboranyl porphyrin.

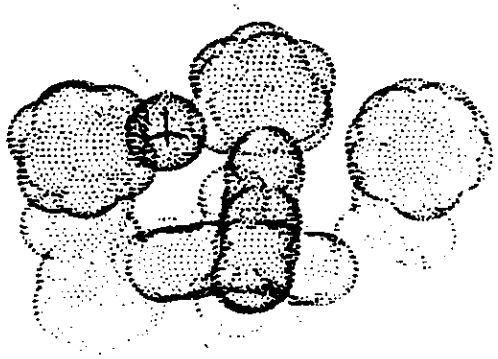

Figure 10.

Various other modified metalloporphyrins have been evaluated by molecular mechanics calculations. Several of these are currently being synthesized.

Synthesis. After a potential metalloporphyrin catalyst such as the carboranyl porphyrin has been evaluated by CAMD methods, it must be synthesized and tested. Computer designed metal-porphyrins with shape and size selective cavities at the metal site have been synthesized. In collaboration with S. B. Kahl at the University of California at San Francisco, the manganese(III) derivative of the long-chain carboranyl porphyrin (with a carbon atom in the amide links, see Figure 18) has been synthesized.

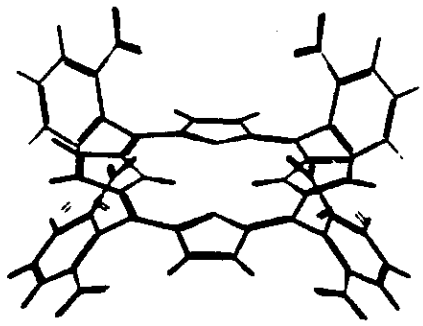

Figure 11.

Some potential problems with this catalyst involve (1) the prevention of the reaction from occurring at the un-protected face of the porphyrin, and (2) the rotation of the phenyls so that the carborane cages no longer

form a cavity. Both of these problems might be solved if the carboranyl analog with carboranes attached at all 8 ortho-phanyl position could be synthesized. The octa-carboranyl porphyrin would have both axial coordination positions of the metal protected. (See Figure 12.)

Tetra(o-dinitrophenyl)porphyrin (TDNPP) has recently been synthesized at Sandia.[2] This porphyrin, shown in Figure 11, is the precursor for bis-deep-pocket porphyrins like the carboranyl porphyrin shown in Figure 12.

Figure 12.

Structural Characterization. Characterization of the synthesized designed catalysts is a major task of the CAMD program. For example, TDNPP has been characterized by laser-desorption FT mass spectrometry and by various spectroscopic techniques including Raman-difference, NMR, FTIR and UV-visible absorption spectroscopies. Mass spectrometry shows that the putative TDNPP compound has the correct molecular weight (795 amu).[2]

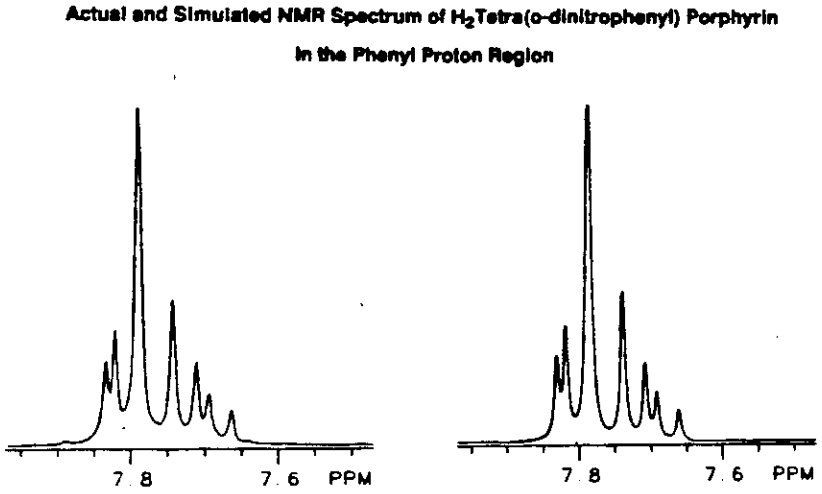

Figure 13.

Figure 13 shows the phenyl-proton region of the NMR spectrum of the putative TDNPP compound.[2] The spectrum on the left is the actual spectrum; the one on the right is a simulation. The simulation is obtained by assuming an AB_2 proton spectrum with an 8 Hz coupling between A (para) and B (meta or ortho) protons. The AB_2 spectral pattern implies that the phenyl rings are substituted at either both ortho or both meta carbons; the size of the coupling constant implies that the A and B protons are at adjacent positions on the ring. Therefore, the phenyl rings have substituents at both carbons ortho to the carbon bonded to the porphyrin macrocycle.

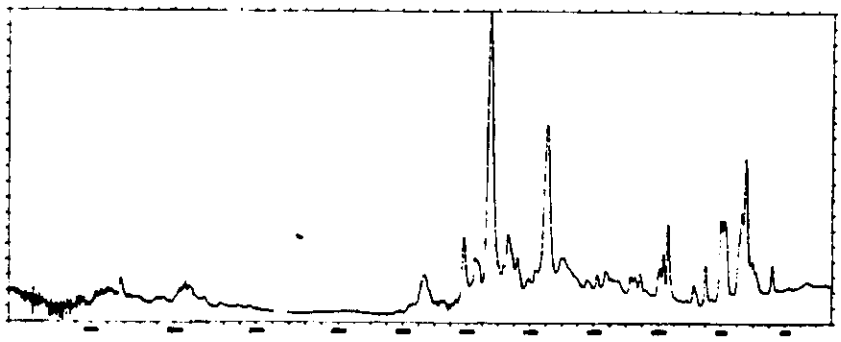

Figure 14.

The FTIR spectrum, shown in Figure 14, indicates that the ortho substituents are nitro groups.[2] The N=O symmetric and antisymmetric stretching vibrations give the two strong lines at 1345 and 1525 cm^{-1}. Further, these lines disappear when the nitro groups are converted to the

amines. They are replaced by the amine deformation at 1612 and the symmetric and antisymmetric N-H stretching at 3461 and 3369 cm^{-1}.

Alkane-Oxidation Catalytic Activity. Several activity testing goals have been pursued. First, methane conversion to methanol using metalloporphyrin catalysts should be demonstrated. Second, a stable process using O_2 as the oxidant needs to be developed. Third, a photochemical cycle that provides the reductant (for activating O_2) is desirable. And, finally, we would like to show regio-selective hydroxylation of alkanes using the designed sterically hindered catalysts. Progress has been made toward achieving these goals and the results are described in the next section.

SIGNIFICANT ACCOMPLISHMENTS: **Methane Conversion.** We have demonstrated that an iron porphyrin will catalyze the hydroxylation of methane and ethane. Table 1 compares the reaction conditions under which methane, ethane, and hexane are converted to the corresponding alcohols. The batch reactions were run under ambient conditions except that the gaseous hydrocarbons were run at elevated pressures to increase solubility. For simplicity in interpretation, the catalyst used in this work is not one of the designed catalysts, but a sterically un-hindered one (Fe tetra(pentafluorophenyl)porphyrin). Iodosylbenzene was used as the oxidant.

LOW MOLECULAR WEIGHT ALKANE CONVERSION TO ALCOHOLS

- Methane

  Reaction Conditions:
  - Oxidant - Iodosylbenzene (0.1 mmoles)
  - Solvent - C_6F_5Cl
  - Pressure - 1200 psig
  - Catalyst - $FeTF_5PPCl$ (0.2 umoles)
  - Reaction volume - 2 ml
  - Reaction time - 3 hr
  - Temperature - 25° C

  Yield (Methanol):
  - Catalyst Turnovers - 0.1 (Rubidium - 0.01)
  - Percent Oxidant - 0.02%

- Ethane

  Reaction Conditions:
  - Same as for Methane except:
  - Pressure - 840 psig
  - Reaction time - 4 hr
  - Solvent - Benzene

  Yield (Ethanol):
  - Catalyst Turnovers - 3.3 (Rubidium - 0.2)
  - Percent Oxidant - 0.7%

- Hexane

  Reaction Conditions:
  - Oxidant - Iodosylbenzene (0.1 mmoles)
  - Solvent - Methylene Chloride
  - Pressure - Ambient
  - Catalyst - $FeTF_5PPCl$ (0.05 umoles)
  - Reaction volume - 2 ml
  - Reaction time - 2 hr
  - Temperature - 25° C

  Yield (Hexanols):
  - Catalyst Turnovers - 1,100
  - Percent Oxidant - 83%

Table 1.

Hexane is hydroxylated at moderate rates (~9 catalyst turnovers/min for hexanols) to give mainly 2-, and 3-hexanol and some 1-hexanol and hexanones. Ethane is converted catalytically (~3 catalyst turnovers), but much less efficiently. Small amounts of methane were converted also (~0.1 catalyst turnovers), but even less effectively. These results compare favorably with recent Russian work[3] using a different Fe porphyrin (Fe(III) tetra(o-nitrophenyl)porphyrin). See Figure 15.

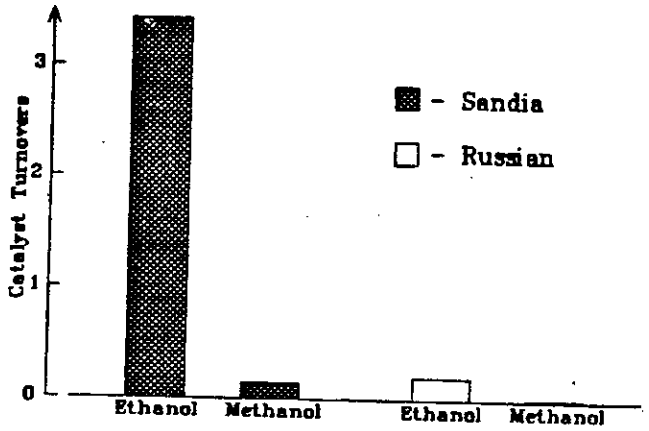

Figure 15.

The product yields are much less than could be expected if a stable oxidant system could be found. For example, note that only 0.02% of the oxidant is converted to give methanol, yet none remained at the end of the reacti n. Even for hexane, only 53% of the oxidant goes into producing hexanols. The low yields in terms of oxidant converted to product can be shown to result from efficient catalytic destruction of the oxidant.

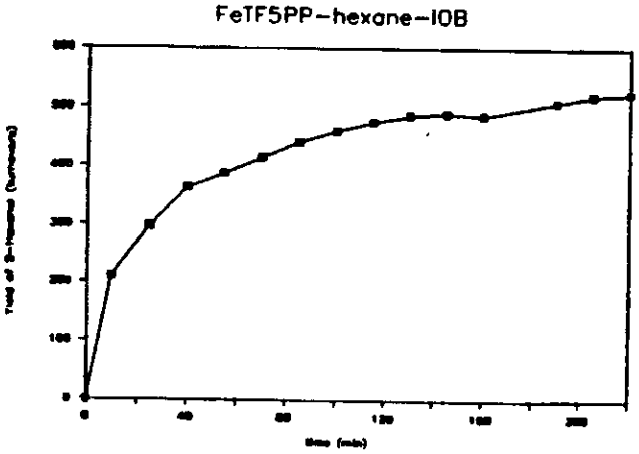

Figure 16.

Figure 16 show the yield of 2-hexanol as a function of reaction time. We see that the reaction rate is initially high, but drops off rapidly with

time. This behavior is shown to result from depletion of oxidant both by conversion of hexane and by catalytic destruction of oxidant (see below).

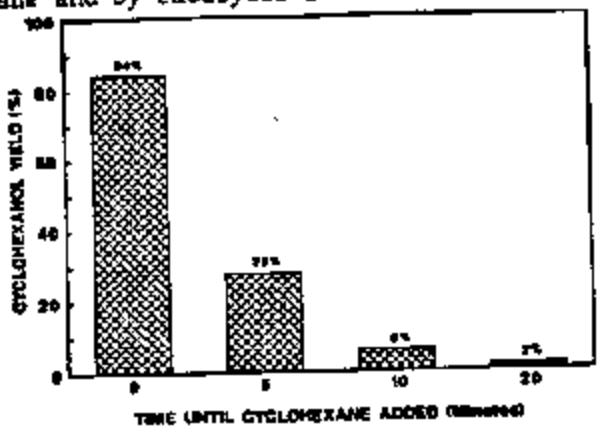

Figure 17.

The degree of destruction of oxidant is illustrated in Figure 17. At zero time the reaction is initiated in the absence of alkane substrate, which is subsequently added after various elapsed times. If the oxidant were not catalytically destroyed the time at which the substrate was added would not matter. (The catalyst is not destroyed, as determined from the UV-visible absorption spectrum.) Instead, we see that very little oxidant remains after only 20 min. The reaction is catalytic because the same experiment in which the catalyst and substrate are added after various elapsed times always gives the same cyclohexanol yield.

In the case of methane and ethane conversion, catalytic destruction of the oxidant has a great effect. Because of the lower intrinsic conversion rates for methane and ethane very little is converted during the time when viable oxidant is present. The difference in the conversion rate is exaggerated for the alkanes, because hexane and cyclohexane compete favorably with oxidant inactivation whereas methane and ethane do not.

The oxidant-inactivation problem should be amenable to catalyst design efforts, since it is possible that a protected cavity can be devised which allows oxygen transfer from iodosylbenzene to the Fe, but which does not allow the active Fe-porphyrin intermediate to attack iodosylbenzene via the destructive pathway.

Activity Tests with Designed Catalysts. Several designed porphyrins have been synthesized and characterized spectroscopically (see above) and have also been chemically characterized and tested for alkane activation activity. In particular, the long-chain carboranyl porphyrin shown in Figure 18 has been tested. Because the long chain with a carbon atom between the amide group and the carborane is more flexible than when the extra atom is an oxygen, the pocket tends to collapse (compare Figure 18

and Figures 9 and 10). Nevertheless, one Mn axial coordination site is fairly protected (Figure 18), and the calculations predict some degree of regio-selectivity in alkane oxidation reactions.

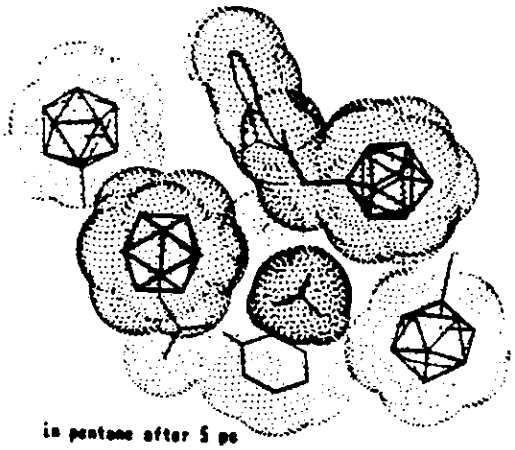

Figure 18.

To determine the regio-selectivity of alkane oxidation at the protected site, we must somehow block the reaction at the unprotected face of the porphyrin. One method is to bind a ligand at that position. Figure 19 shows the result of a UV-visible absorption spectroscopic study of the binding of imidazole to a completely unhindered Mn porphyrin. Assuming that only one imidazole binds per Mn porphyrin gives a poor theoretical fit to the binding data. However, assuming two imidazoles bind gives a good fit, a shown in Figure 19.

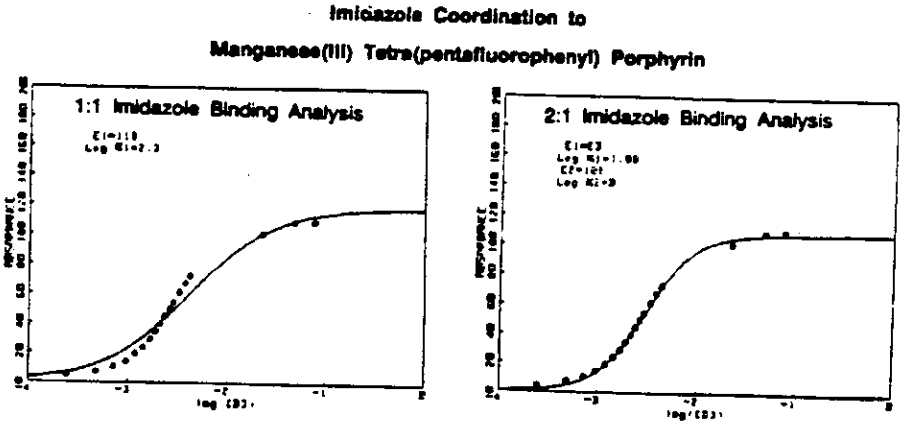

Figure 19.

Studies of the catalytic activity as a function of imidazole concentration show that the 1:1 complex is active whereas the 2:1 complex is inactive. This is deduced from the fact that peak activity occurs at

the concentration of the imidazole at which the concentration of the 1:1 complex is greatest. See Figure 20.

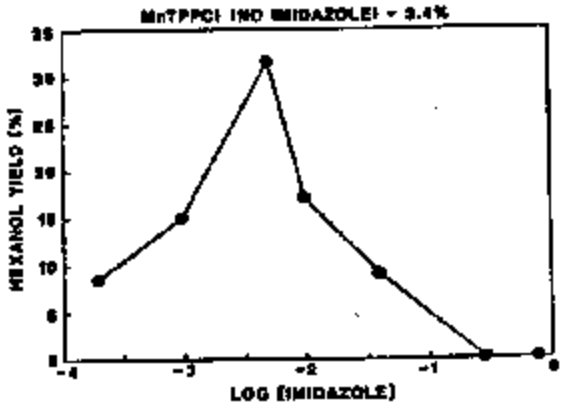

Figure 20.

For the carboranyl porphyrin (MnTCBPP), a similar analysis of imidazole binding (shown in Figure 21) indicates that only the 1:1 complex is formed. This has two advantages. First, imidazole can be used to block the unprotected coordination site. Second, imidazole acts as a promoter (see Figure 20), raising the catalytic activity at the protected Mn site. Furthermore, we obtain complete formation of the most active 1:1 complex, rather than less than 20% formation of the 1:1 complex for sterically unhindered porphyrins like $MnTF_5PP$.

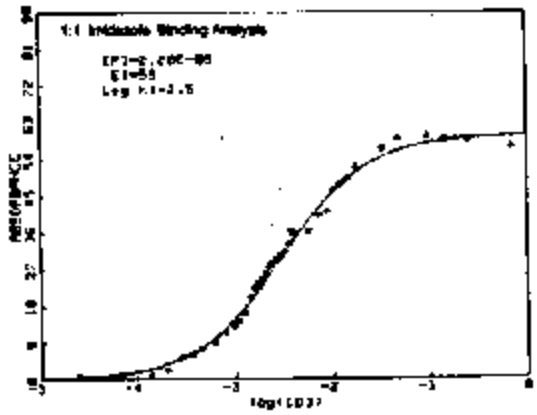

Figure 21.

Figure 22 summarizes the results of the activity testing for the carboranyl-porphyrin catalyst. The first bar shows the yield of hexanol for $MnTF_5PP$ for comparison with the results for the designed carboranyl porphyrin. The second bar gives the cyclohexanol yield for MnTCBPP in the absence of imidazole (Im). Without imidazole present the reaction is free

to occur at the unprotected face of the porphyrin and a moderate yield is observed. When imidazole is present only the residual cyclohexanol formed even in the absence of catalyst is observed (third bar). The lack of catalysis in this case is a result of the limited access that iodosylbenzene and cyclohexane have to the pocket on the sterically hindered face of the porphyrin.

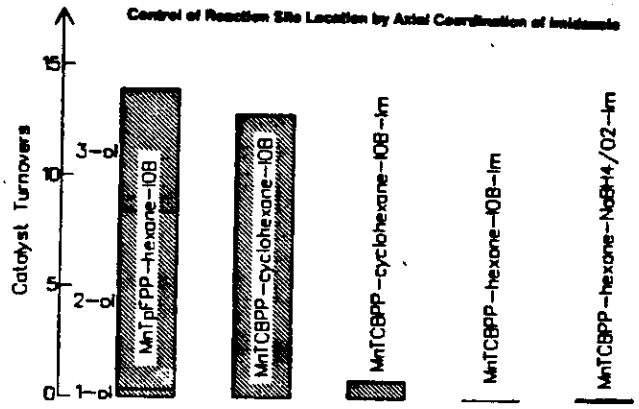

Figure 22.

On the other hand, n-hexane is predicted to have greater access to the cavity and might be expected to be oxidized especially at the end carbon positions. Hexane is not oxidized significantly (fourth bar) presumably because the oxidant is still too large to enter the pocket.

A smaller oxidant such as O_2 can enter the pocket, and, therefore would be expected to oxidize hexane. Indeed, hexane is hydroxylated when O_2 is used as he oxidant (last bar). Further, selectivity for 1-hexanol over the secondary hexanols is indicated. However, the latter result needs to be confirmed using a longer lived oxidant system than the sodium borohydride/O_2 system.

Photochemical O_2-Oxidation of Alkanes. A goal is to develop a long-lived system using O_2 as the oxidant, preferably a photochemically initiated system. A photochemical system would allow mechanistic and reaction-rate studies. In the past, strong reductants such as sodium borohydride, H_2, and Zn metal have been used. These compounds provide the reducing equivalents (e^- in Figure 1) required to reduce the Fe(III) porphyrin and the O_2-Fe(II)-porphyrin complex in the P_{450} cycle. However, these reductants suffer in that they must be replenished periodically, or, in the case of H_2, the required Pt colloid catalyst is expensive and unstable. All are short lived systems.

A photochemical cycle that drives alkane oxidation has been developed. The photochemical system has the advantage that it is long lived (>6 hr) and can be photo-initiated for spectroscopic determinations of reaction

rates. The system mimics biological photosynthesis and electron-transfer processes to drive biomimetic hydrocarbon oxidation. The photochemical cycle is illustrated in Figure 23.

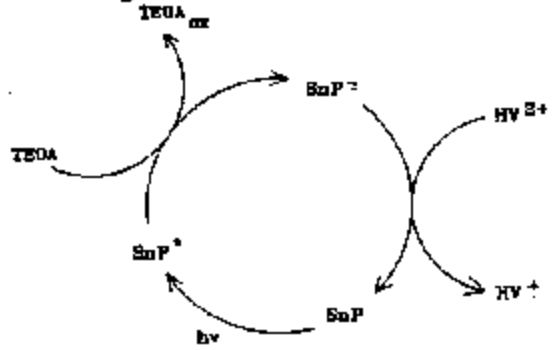

BIOMIMETIC PHOTOSYNTHESIS OF REDUCING EQUIVALENTS
Figure 23.

The photochemical process was developed and patented at Sandia for photochemical splitting of water to generate H_2.* However, the cycle can be used to photochemically convert a weak sacrificial reductant, such as a tertiary amine (E = +0.8 V), to a strong reductant (triathanolamine, TEOA), such as the Sn-porphyrin π-anion or reduced heptylviologen (E = -0.5 V). Essentially, the reaction uses visible light energy to activate O_2 rather than high temperatures as in conventional direct methane conversion schemes. The full reaction scheme for photochemical oxidation of hydrocarbons is shown in Figure 24. A tin(IV) or antimony(V) porphyrin is used as the photosensitizer.

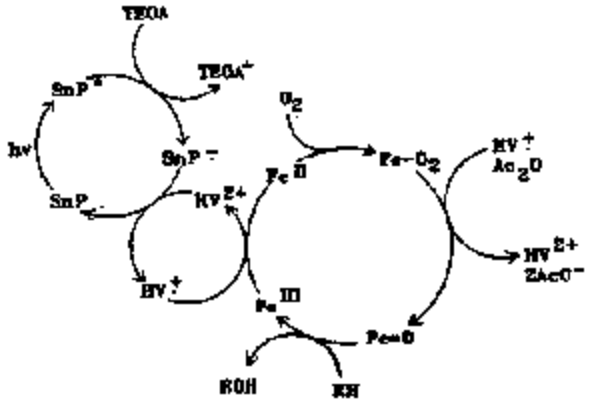

Figure 24.

Figure 25 shows the hexanol yield in terms of photosensitizer turnovers as a function of reaction time. The system shows little degradation even during 6 hr. After 6 hr the catalyst had turned over 46 times.

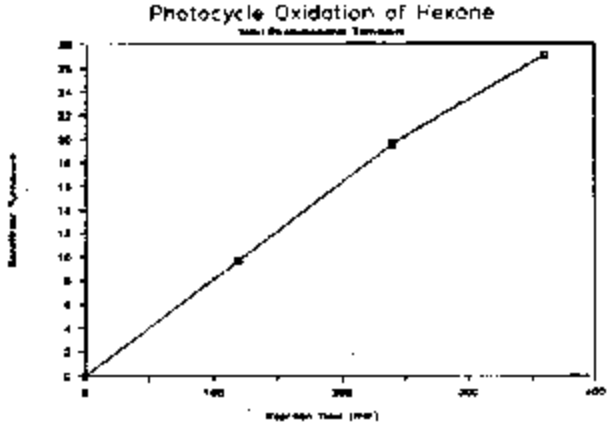

Figure 25.

References

1. Poulos, T. L.; Finzel, B. C.; Gunsalus, I. C.; Wagner, G. C.; Kraut, J., J. Biol. Chem. 1985, 260, 16122.
2. Quintana, C. A.; Aasink, R. A.; Shelnutt, J. A., Inorg. Chem. 1988, submitted.
3. Belova, V. S.; Khenkin, A. M.; Shilov, A. E., Kinet. Katal. 1987, 28, 10[illegible].
4. (a) Shelnutt, J. A., J. Am. Chem. Soc. 1983, 105, 7179. (b) Shelnutt, J. A., U. S. Patent 4,568,435, 1986. (c) Kalyanasundarum, K.; Shelnutt, J. A.; Gratzel, M., Inorg. Chem. 1988, 27, 2820.

PUBLICATIONS: (1) "Computer-Aided Molecular Design of Alkane-Activation Catalysts," J. A. Shelnutt; F. V. Stohl; B. Granoff, ACS Fuel Chem. Div. Preprints, 33, 479 (1988). (2) "The Design of Methane Activation Catalysts," F. V. Stohl; J. A. Shelnutt; B. Granoff, Proc. 9th Intl. Cong. Cat., Vol. 2, eds. M. J. Phillips; M. Ternan (Chem. Inst. Canada) pg. 982, (1988). (3) "Sensitization and Photoredox Reactions of Zn(II)- and Sb(V)(O)(Cl)-Uroporphyrins in Aqueous Media," K. Kalyanasundarum; J. A. Shelnutt; M. Gratzel, Inorg. Chem. 27, 2820 (1988). (4) "Resonance Raman Spectroscopic Investigation of Axial Coordination in *M. thermoautotrophicum* Methyl Reductase and Nickel Tetrapyrrole Cofactor F_{430}," A. R. Shiemke; R. A. Scott; J. A. Shelnutt, J. Am. Chem. Soc. 110, 1645 (1988).